



Alternation and interchange of $e/4$ and $e/2$ period interference oscillations consistent with filling factor $5/2$ non-Abelian quasiparticles

R. L. Willett,* L. N. Pfeiffer, and K. W. West

Bell Laboratories, Alcatel-Lucent, 600 Mountain Avenue, Murray Hill, New Jersey 07974, USA

(Received 15 December 2009; revised manuscript received 11 August 2010; published 1 November 2010)

It is a theoretical conjecture that $5/2$ fractional quantum Hall state charge $e/4$ excitations may obey non-Abelian statistics. In edge state interference these purported non-Abelian quasiparticles should display period $e/4$ Aharonov-Bohm oscillations if the interfering quasiparticle encircles an even number of localized $e/4$ charges but suppression of oscillations if an odd number is encircled. To test this hypothesis, here we perform swept area interference measurements at $5/2$. We observe an alternating pattern of $e/4$ and $e/2$ period oscillations in resistance for a large change in the interferometer area, with the area sweep changing the number of enclosed localized $e/4$ quasiparticles. This aperiodic alternation is consistent with proposed non-Abelian properties: the $e/4$ oscillations occur for encircling an even number of localized quasiparticles, and the lower amplitude $e/2$ oscillations are observed when encircling an odd number. The large amplitude $e/4$ oscillations dominate the measurement when the localized quasiparticle number is even, but at odd number they are suppressed, allowing observation of the smaller $e/2$ oscillations that may be persistent throughout the measurement. The aperiodic alternation corresponds to the area sweep sampling an expected aperiodic spatial distribution of localized quasiparticles. Importantly, adding localized quasiparticles to the encircled area by changing magnetic field can change the parity of the enclosed quasiparticle number and should induce interchange of the expressed $e/4$ and $e/2$ periods: just such interchange of the $e/4$ and $e/2$ oscillation periods is observed in measurements presented here, with agreement between the measured and calculated values of B field necessary to add a single quasiparticle to the interferometer area. These results are specifically consistent with proposed non-Abelian $e/4$ quasiparticle properties.

DOI: [10.1103/PhysRevB.82.205301](https://doi.org/10.1103/PhysRevB.82.205301)

PACS number(s): 73.43.Fj

I. INTRODUCTION

The enigmatic fractional quantum Hall effect (FQHE) state at $5/2$ filling factor¹⁻⁷ may possess excitations that obey non-Abelian statistics.^{2,6-8} If this is indeed true, these excitations may then be employable in performing topological quantum computation operations.⁹

It has long been postulated that the quasiparticle excitations in the fractional quantum Hall effect have nontrivial braiding statistics,¹⁰ with these quasiparticle charges and statistics potentially measurable in interference experiments.¹¹⁻¹⁵ With respect to the $5/2$ state, theory has been proposed¹⁶⁻²⁰ that an interference experiment may be able to discern its statistics; if $5/2$ quasiparticles can be made to encircle flux quanta and localized quasiparticles in an interference device, a distinctive pattern should result if the quasiparticles are non-Abelian. For an even number of encircled, localized particles, $e/4$ period Aharonov-Bohm (A-B) oscillations should result. However, if an odd number of quasiparticles are encircled these oscillations will be suppressed. Experimentally, interferometry of FQHE edge states, and in particular $5/2$, has been accomplished recently.²¹ The finding of interference periods consistent with $e/4$ charge in that study corroborates reports of the determination of $5/2$ excitation charge^{22,23} but charge determination does not define the statistics of the excitations. The question of the $5/2$ quasiparticle statistics warrants an interference measurement that demonstrates the consequence of enclosing even and odd numbers of quasiparticles.

We report here interference measurements at filling factor $\nu=5/2$ that address this hypothesis. An interferometer with

an adjustable side gate is used that changes the encircled area, changing the number of enclosed flux quanta, and for large enough excursion changes the number of encircled, localized quasiparticles. We observe for large gate excursions an aperiodic alternation of interference patterns; a distinct $e/4$ period oscillation alternates with a distinct $e/2$ period oscillation. This alternation can be effected by addition of magnetic flux, and its consequent quasiparticle number change, whereby the $e/4$ and $e/2$ periods interchange. These results are specifically consistent with non-Abelian $e/4$ quasiparticle properties in the response to both B -field application and gate excursion. The $e/4$ oscillations represent the prescribed encircling of an even number of localized quasiparticles. The alternate $e/2$ oscillations are observed when the encircled area contains an odd number of quasiparticles as the $e/4$ oscillations are suppressed. The alternation pattern is exposed for sufficiently large area sweeps; the aperiodic pattern corresponds to the expected random spatial distribution of localized quasiparticles within the swept area. Importantly, these specific aperiodic patterns can be induced to interchange the $e/4$ and $e/2$ periods upon addition of magnetic field corresponding to addition of a single localized $e/4$ quasiparticle. The observation of both the alternation and interchange of $e/4$ and $e/2$ periods specifically supports the conclusion of non-Abelian statistics for the $e/4$ quasiparticle.

II. EXPERIMENTAL

A. Experimental overview

High-mobility, high-density heterostructures of fixed density n access filling factors $\nu=n\hbar/eB$ through swept mag-

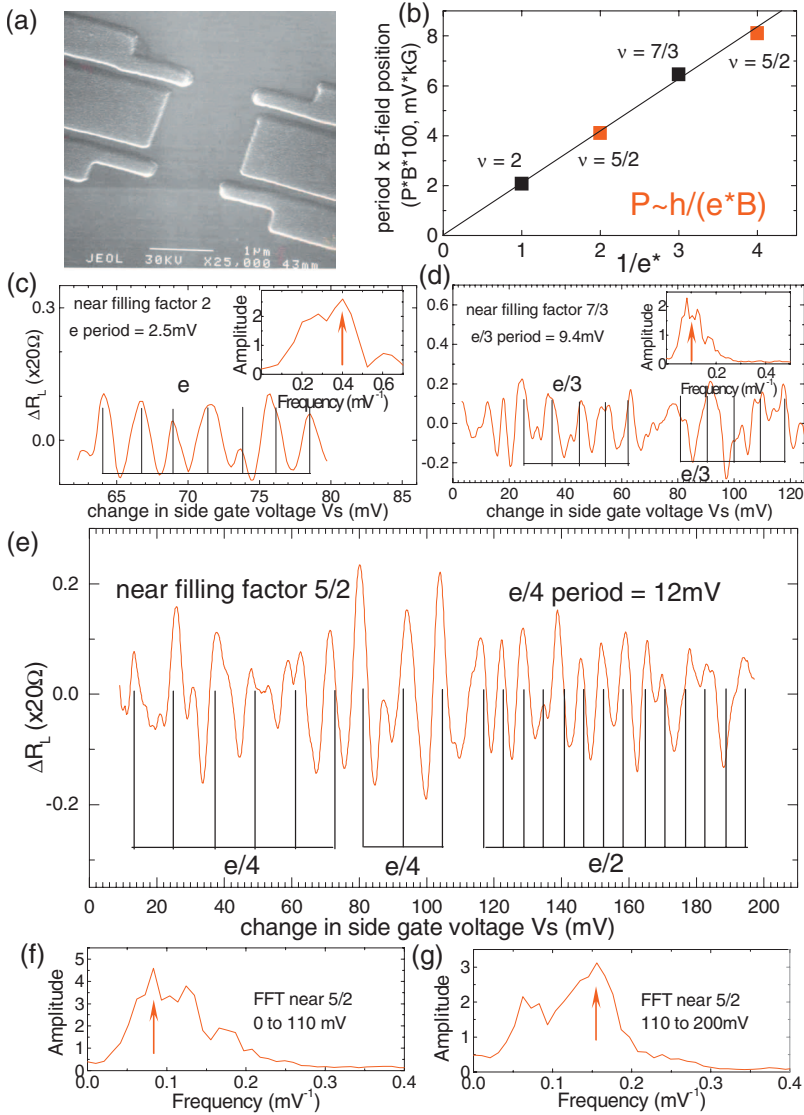


FIG. 1. (Color) Interference device and Aharonov-Bohm oscillations at multiple filling factors, showing $e/4$ and $e/2$ periods near $5/2$. Panel a is the device electron micrograph. Panels (c)–(e): ΔR_L versus side-gate sweep ΔV_s , showing A-B oscillations at filling factors $\nu=2$, $7/3$, and $5/2$. Vertical lines in the $\nu=2$ and $\nu=7/3$ traces are consistent with the peaks of their respective FFTs of the spectra (c and d insets). In A-B oscillations the period is dependent on quasiparticle charge e^* and magnetic field B with period $\sim \Delta V_s \sim \Delta A \sim (h/e^*)/B$. In panel b measured period $\times B$ is plotted against the assumed charge for $\nu=2$ and $7/3$ of e and $e/3$, respectively; the data are consistent with A-B oscillations. Panel e: ΔR_L versus side-gate sweep ΔV_s for the same sample preparation at $5/2$ shows two periods corresponding to quasiparticle charge $e/4$ and $e/2$ periods. Vertical lines marking these periods are consistent with FFT peaks taken over the range at which each predominates (panels f and g). Charge periods $e/4$ and $e/2$ are consistent with A-B oscillations as shown by the inclusion of their measured period and B products in Fig. 1(b): the measured periods agree with the expected values for charges $e/2$ and $e/4$. Data taken at $T=25$ mK, and drive current 2 nA, sample preparation a. All swept gate data displayed in this study are measured on the high B -field side of the indicated filling factor and for the fractional states within kG of the minimum.

netic field B . The interferometer, shown in Fig. 1(a) and schematically in Fig. 2(a), is composed of two quantum point contacts (qpc) and a central channel region. Each component is independently controllable.^{21,24} The confinement device is an aluminum top gate structure, with details outlined below. Transport is measured through the devices with R_L (Ref. 25) as defined in Fig. 2; typical bulk and R_L magnetotransport are also displayed in Fig. 2. The qpc's voltages are adjusted beyond full depletion to promote preservation of the $5/2$ state in the interferometer, and the side-gate voltage V_s is independently varied to change the enclosed area.

A-B oscillations will occur when the side-gate voltage is varied, with the period $P \sim \Delta V_s \sim \Delta A \sim (h/e^*)/B$, V_s the side-gate voltage, A the enclosed interferometer area, e^* the interfering charge value, and B the magnetic field. Side-gate voltage sweeps will change the enclosed number of flux quanta resulting in periods defined by this dependence on e^* and B . As noted in prior work the period measured at $\nu=2$ with $e^*=1$ and at $\nu=5/3$ or $7/3$ with $e^*=e/3$ and their respective B -field values can be used to derive the proportionality to establish the expected period for $5/2$. This interference and successful determination of oscillation periods for

multiple FQHE states has been demonstrated previously.²¹ Oscillation periods at $5/2$ consistent with $e^*=e/4$ and $e/2$ were demonstrated in these studies over small V_s excursions.

The experimental focus in this study is on (a) preparation of the sample to optimize observation of the $e/4$ and $e/2$ oscillations, (b) markedly expanding the range of the V_s 's sweeps compared to previous studies²¹ to determine the relative prevalence of the $e/4$ and $e/2$ oscillations, and (c) examining the B -field dependence of the $e/4$ and $e/2$ oscillations near $5/2$. As shown below, expanding the range of V_s sweep reveals $e/4$ and $e/2$ oscillation periods that are observed to alternate aperiodically. This alternation can then be made to interchange $e/4$ and $e/2$ periods with change in B field corresponding to the addition of a single localized quasiparticle.

B. Device preparation and measurement details

High-mobility, high-density heterostructures with Ni/Au/Ge contacts diffused into the mesa edge are used here as in previous measurements.^{21,24} The heterostructures are of fixed density n away from the top gate structures, with filling factors $\nu=nh/eB$ adjustable through sweep of the magnetic

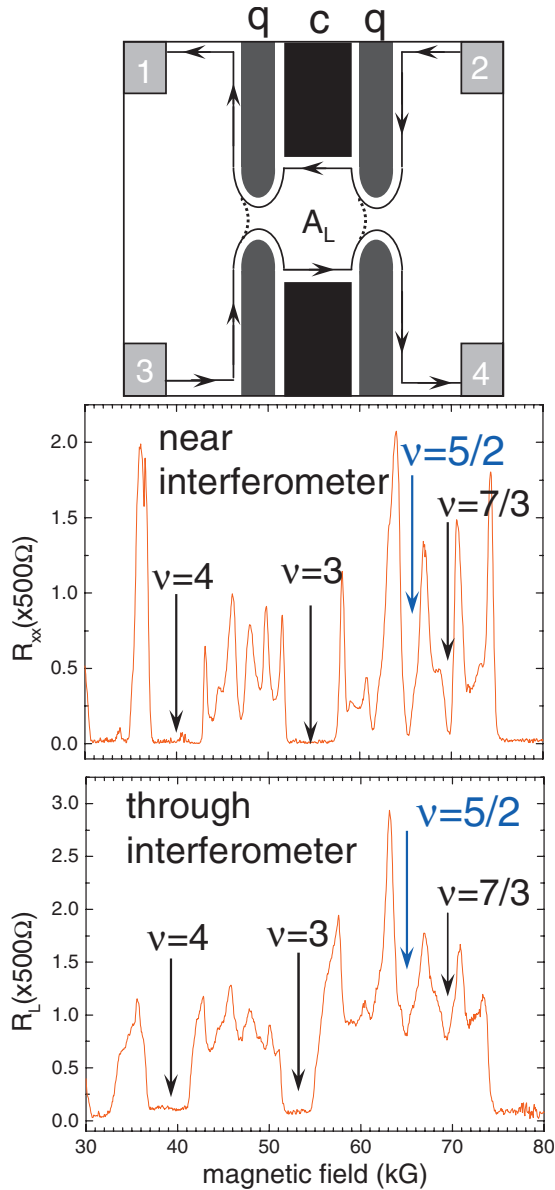


FIG. 2. (Color) Four terminal resistance near and through the interferometric device. Top panel is a schematic of the interference device: confined area A_L is defined by top gates q , quantum point contacts, and the central channel gate c , with voltage V_s . Change in V_s independently controls the interferometer area A . R_L measurement uses drive current from contacts 1 to 2 and voltage drop from 3 to 4. Middle panel is longitudinal resistance measured adjacent to the interferometric device in the bulk of the 2D electron system. Bottom panel is R_L measured across the device. $T=25$ mK, current 2 nA, sample preparation b.

field B . The interferometer is a top gate structure with biasing able to deplete the underlying two-dimensional (2D) electron system and adjust the 2D electron density laterally adjacent to the gates. It is shown schematically in Fig. 2(a), and is composed of two qpcs and a central channel region. Each component is independently controllable, with previous studies^{21,24} detailing the operation of the device and its components. The 2D electron gas is approximately 200 nm below the heterostructure surface. A 40nm SiN layer on the surface

of the heterostructure further separates the 2D electron gas from the ~ 50 nm thick Al top gates. These gates fully deplete the underlying 2D electron gas at about -2.5 V; this top gate structure is displayed in the electron micrograph in Fig. 1(a). Transport is measured through the devices using standard lock-in techniques (see below), with R_L (Ref. 25) as defined in Fig. 2(a). The samples are illuminated with a red light-emitting diode (LED) at low temperatures, down to 25mK in a dilution refrigerator.

Data displayed in this study include results from a total of eight sample cool downs (room temperature to 25 mK) with multiple illuminations within each cool down. The red LED illumination empirically serves to enhance the sample mobility and induces differences in the sample conduction, even in bulk transport examinations. These illuminations therefore produce a nominally different sample preparation with each illumination cycle.

The experiments are conducted in a window of qpc operation of sufficiently low bias that allows the FQHE states to exist, particularly the $5/2$ state, but large enough bias to observe interference. This principal is discussed below.

A fundamental aspect of these experiments is that the interferometer is to be operated such that the fragile fractional quantum Hall states at $5/2$, $7/3$, etc., are preserved within the device, yet sufficient backscattering must be induced to see quasiparticle interference. The backscattering is produced at the qpcs, where ideally a path of density uniform with the bulk is maintained and backscattering occurs across this density. Inducing this backscattering for integral quantum Hall states where the energy gaps are >10 K is readily achievable given those states are robust against density perturbations: the edges can be brought into close proximity to achieve high backscatter rates across a small tunneling dimension. This is not the case for the fragile FQHE states with gaps two orders of magnitude smaller: the qpcs must be kept open to sustain the bulk density in the gap (while still fully depleting beneath the gate), and the tunneling must therefore occur over a larger dimension. This larger tunneling distance is probably the root of the small amplitude, phase interrupted interference pattern that is observed in this study. The similar interference noted for the integers as for the fractions reflects the fact that the tunneling is occurring over the same gate biases: in all measurements here the qpcs are maintained at the same biases when comparing integer and fractional states in order to retain the dimension A of the interferometer. Large biases on the qpcs would induce better integral state interference but damage the FQHE states.

The sample preparation involves a procedure of charging the gates, then allowing the system to equilibrate. The oscillatory features at FQHE states at $5/3$, $7/3$, and $5/2$ filling factor are improved with a period of equilibration of several days. This procedure, in addition to noise reduction efforts, have allowed closer examination of the interference of FQHE states compared to previous work.²¹ Experimental modifications and procedures were also undertaken from previous experiments to allow large side-gate excursion.

Small signal sensitivity is achieved by very slow sweep of the side gate (ΔV_s) at rates typically of ~ 400 mV/24 h using long time constants (30–100 s) in the lock-ins and the data are averaged as taken over 0.2 mV wide bins; different

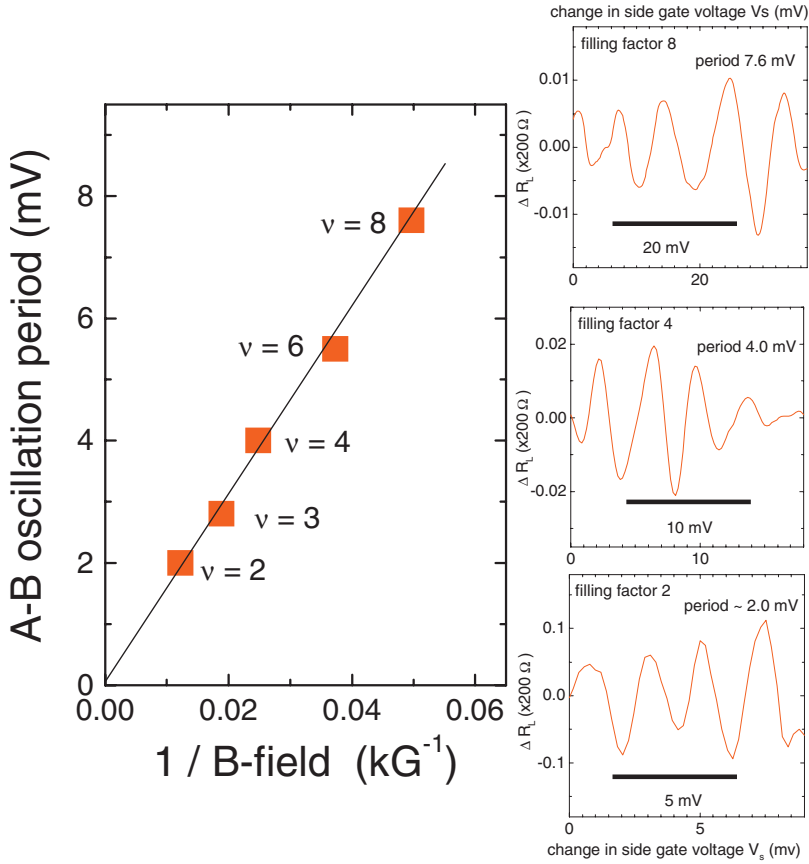


FIG. 3. (Color) Aharonov-Bohm oscillation periods for magnetic field values near integer filling factors of 2, 3, 4, 6, and 8. The periods increase inversely as $1/B$, as expected for A-B oscillations in which oscillation period $\sim (h/e^*)/B$. Sample ΔR_L measurements are displayed in the right-side panels, noting that the V_s axis is changing by a multiple of 2 in the progression. These results are inconsistent with Coulomb blockade but are as expected for A-B oscillations; see results of Ref. 26. Additionally, measurements of oscillations at different integers for swept B -field show no change in period over this filling factor range, also consistent with A-B oscillations. $T = 25$ mK, $I = 1$ nA, sample preparation c.

traces cannot be averaged due to phase changes between sweeps, however the collected data are averaged instrumentally using this standard technique.

III. RESULTS

A. Aharonov-Bohm interference measurements and charge determination

In Fig. 1 interference patterns are studied at a series of filling factors. In panel c, transmission resistance ΔR_L is plotted against side-gate voltage change at filling factor $\nu = 2$. ΔR_L is the measured resistance with the gross background subtracted. As observed previously,²¹ A-B oscillatory features are present in ΔR_L with the dominant periodicity marked by vertical lines. The period of these vertical lines is determined by the spectral peak of a fast Fourier transform (FFT) performed on the ΔR_L data of Fig. 1(c); the inset displays the FFT result. This period of A-B oscillations is then used with the relationship $P \sim \Delta V_s \sim \Delta A = (h/e^*)/B$; assigning $e^* = e$ for $\nu = 2$, the period for other filling factors can be derived using their expected charges. Such a derivation is made for the filling factor $\nu = 7/3$, necessarily using both $e^* = e/3$ and the B -field values of the respective measurements near $\nu = 2$ and $\nu = 7/3$. ΔR_L is then measured versus change in side-gate voltage near filling factor $7/3$, with results displayed in Fig. 1(d). The vertical lines of panel 1d reflect the derived periodicity, and the A-B oscillations marked $e/3$ in the data at $7/3$ are in agreement with that periodicity. This period is further corroborated by the spec-

tral peak of an FFT performed on the Fig. 1(d) ΔR_L data: see inset. The $\nu = 2$ and $7/3$ FFT spectra periods are plotted in panel 1b, demonstrating the proportionality of the product of the period and the B -field position of the measurement versus the inverse charge. A property of the interference oscillations observed with these interferometers as noted in previous studies²¹ is that they occur in series with phase disruptions. To delineate the series of phase coherent oscillations, in all ΔR_L data the charge is marked for each coherent section: for example, Fig. 1(d) has two coherent sections marked $e/3$.

The potential for interferometer resistance oscillations to be due to Coulomb blockade (C-B) rather than A-B interference has been studied,²⁶ particularly for small interferometers similar to those used here. This possibility is contradicted here by the period dependence of Fig. 1(d) and also in interference results at a series of integer quantum Hall states from 2 to 8, with data demonstrated in Fig. 3. At integer ν , contrary to the B -independent period demonstrated in C-B dominated interferometers,²⁶ the oscillation periods of this study demonstrate linear increase with $1/B$ in side-gate sweep measurements as specifically expected for A-B oscillations with a single charge; see figure. In addition, for swept B -field measurements, oscillations with B -field period independent of ν are observed near these integer filling factors, again consistent with A-B oscillations and contrary to the properties of Coulomb blockade. The presence of A-B oscillations and not Coulomb blockade in this study may be attributed to the open geometry of the quantum point contacts of the devices employed here.

Focus now centers on resistance ΔR_L data taken near filling factor $5/2$, and as shown previously²¹ A-B oscillations

are observed that are consistent with $e/4$ and $e/2$ charges. A typical interferometer resistance trace is shown in panel 1e, where two predominant periods present serially as the side gate is swept. From V_s change of 0 to 110 mV a larger period oscillation is present, and FFT of this range is shown in panel 1f. This period, as determined from the FFT peak, is consistent with A-B oscillations of charge $e/4$: the product of period and B -field position are plotted in panel 1b and fall in line with the $\nu=2$ and $7/3$ periods. The ΔR_L data section of smaller period (110–200 mV) and the peak of the FFT spectrum taken here (panel 1g) display a period consistent with $e/2$, also plotted in 1b.

B. Alternation of $e/4$ and $e/2$ Aharonov-Bohm periods

Alternation between $e/4$ and $e/2$ oscillations is evident in the results of Fig. 4 demonstrating further examples of resistance measurements across the interferometer near $5/2$ filling. Data from three different sample preparations are displayed, including resistance ΔR_L data, FFTs of these resistance measurements, and additionally plots of the differences in peak to peak positions versus the change in side-gate voltage. In all ΔR_L data panels the $e/4$ and $e/2$ periods as marked by vertical lines are derived from FFT spectra peaks of the A-B measurements, and are consistent with A-B oscillation periods for their respective sample preparations at $\nu=2$ and $\nu=7/3$ or $5/3$.

Panel (i) of Fig. 4, preparation d, shows resistance ΔR_L versus side-gate voltage and demonstrates distinct $e/4$ oscillations flanked by smaller amplitude $e/2$ oscillations. The data span 140 mV in side-gate sweep and are divided into three sections each with a predominant oscillation period of $e/2$ or $e/4$. Each section and the entire range have FFTs applied with the results in panel (ii). Here the FFT spectrum of the full 140 mV side-gate sweep shows two principal peaks corresponding to $e/4$ and $e/2$ periods. The FFT spectrum of Sec. I shows predominance of the higher frequency peak corresponding to the $e/2$ period oscillations. Section II FFT spectrum shows predominance of the $e/4$ period. Section III FFT shows $e/2$ period almost exclusively. These FFTs of the three separate sections demonstrate that the predominant period alternates between $e/4$ and $e/2$ over this side-gate range. To further examine this alternation panel (iii) shows a plot of the difference in peak positions of adjacent prominent peaks throughout the side-gate sweep extracted from the ΔR_L plot of panel (i). These data are the difference in peak position values of the series of oscillations shown in panel (i); [V_s of peak $(n+1) - V_s$ of peak (n)] versus V_s of peak (n) . These data demonstrate the relatively abrupt switching between the two periods of $e/4$ and $e/2$.

Sample preparation e, Fig. 4, shows another example of this alternation between $e/4$ and $e/2$ periods but with more alternations present. In this side-gate range of roughly 180 mV, the predominant period changes four times. A third example of the $e/4$ and $e/2$ alternation is shown in the data from preparation f.

The data of Fig. 4 are representative of the A-B oscillations present near $5/2$. For all side-gate sweeps of this range examined (V_s excursion of roughly 150 mV or more) and at

lowest temperatures (~ 25 mK), $e/4$ and $e/2$ oscillations are present and an alternation between the periods occurs. Measurements show that for different sample preparations the pattern of alternation and the V_s extent for each $e/2$ or $e/4$ sequence is different. The $e/4$ to $e/2$ alternation is aperiodic in that the extent of the $e/4$ or $e/2$ oscillations is not a fixed range, either within a sample preparation or when comparing two different sample preparations. To further examine this aperiodicity, measurements employing a larger range of ΔV_s are used.

Data from measurements applying a larger range side-gate sweep up to 350 mV are shown in Figs. 5 and 6, again presenting the principal finding of alternation between $e/4$ and $e/2$ oscillations. Shown are the plots of ΔR_L versus change in side-gate voltage, plots of the adjacent peak position differences, and additionally the results of scanned FFTs over the full excursion range of the side-gate sweep. The scanned FFT data are the result of performing an FFT over a window of ~ 30 mV progressing across the side-gate sweep range at ~ 5 mV steps. The data plotted are the values from the FFT spectra at the frequencies corresponding to $e/4$ and $e/2$ A-B periods. The FFTs at the respective $e/4$ and $e/2$ spectra positions are normalized by background values of the full spectra (see data analysis review below).

For the sample preparation shown in Fig. 5, using a side-gate sweep of more than 300 mV, the ΔR_L trace shows five sections of alternating $e/4$ and $e/2$ periods. Assignment of $e/2$ or $e/4$ period is supported by the adjacent peak position plots and by the scanned FFT plots, both demonstrating the alternation in periods. In this data with the larger total V_s excursion, the $e/2$ or $e/4$ oscillation range (e.g., $e/4$, 40–130 mV in this sample preparation) can extend up to and more than 100 mV but neither the $e/2$ or $e/4$ sections are of fixed extent. From these large side-gate sweeps the A-B interference can be summarized as an apparent alternation of $e/2$ and $e/4$ periods occurring aperiodically. Data from two additional sample preparations are presented in Fig. 6.

A crucial property of these $e/4$ and $e/2$ period patterns is that they are reproducible. A large V_s sweep as in Fig. 5 is not reproducible in the detail of the phase of the oscillations but importantly the presence of $e/4$ or $e/2$ sections at a given specific side-gate value is reproducible. This reproducibility of $e/4$ to $e/2$ sequences in longitudinal resistance ΔR_L measurements is shown in Fig. 7. Four side-gate voltage sweeps traversing the same total applied side-gate voltage at the same single fixed B field near filling factor $5/2$ are shown in the figure, each from -3.600 to -3.950 V. Each trace labeled A to D corresponds to slow application (~ -15 mV/h) of bias to the channel gate set V_s over the range of the abscissa with similar return rate to the initial bias value. The $e/2$ and $e/4$ periods are marked for comparison between traces, with an error of starting bias of roughly ± 5 mV between traces. Note that the general pattern of the $e/4$ and $e/2$ sequences is reproducible and maintained in some detail between different traces; all four traces show the same oscillation periods of $e/2$ or $e/4$ for a given total side-gate voltage within the error of the applied starting voltage. Four $e/4$ sequences occur from roughly 0 to 40 mV, 100 to 150 mV, from near 175 to 225 mV, and again at 300 mV. In the 100–150 mV sequence the six peaks are generally in

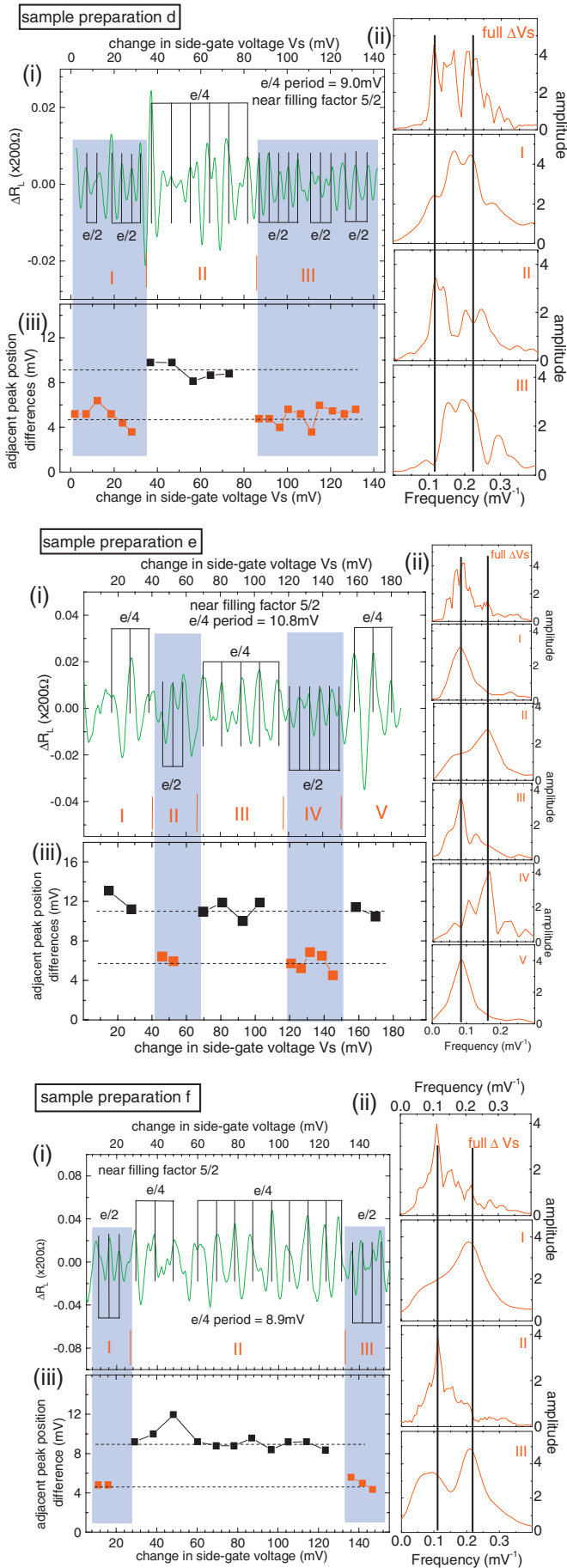


FIG. 4. (Color) Alternation between $e/4$ and $e/2$ period Aharonov-Bohm oscillations near $5/2$ for three sample preparations. Sample preparation d, top, panel (i): near $5/2$, ΔR_L vs ΔV_s for total $\Delta V_s \sim 200$ mV; vertical line periods are from FFT peaks and correspond to $e/4$ and $e/2$ periods as determined by period measurements at filling factors 2, $5/3$, or $7/3$ for each preparation. Within these traces each section showing either $e/2$ or $e/4$ period is numbered and has a respective FFT of that section shown in panel (ii). Panel (ii): respective FFTs of panel (i) sections demonstrating predominance of either $e/4$ or $e/2$ periods in each section. Panel (iii): difference in adjacent predominant peak positions; peak position in side-gate voltage (V_i) is subtracted from the next higher V_s peak position (V_{i+1}), plotting $V_{i+1} - V_i$ vs V_i . Alternation of $e/2$ and $e/4$ oscillation periods is demonstrated in the two predominant adjacent peak position differences. The three sample preparations show different alternation patterns, with preparation e displaying five sections and preparations d and f three sections of $e/4$ and $e/2$ predominance. This alternation can be attributed to change in the parity of the number of quasiparticles enclosed in interferometer area A as V_s is swept to change this area, and the different alternation patterns reflect the distinct spatial patterns of localized quasiparticles in each preparation. $T=25$ mK and current=2 nA in all preparations.

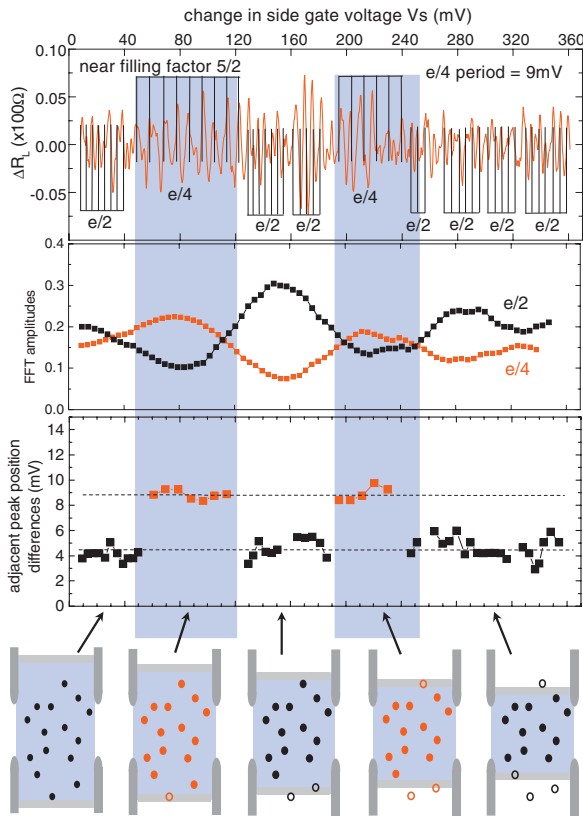


FIG. 5. (Color) Large-range side-gate sweep-induced alternation of $e/4$ and $e/2$ oscillation periods. Displayed are interferometer longitudinal resistance ΔR_L versus change in side-gate voltage, swept window FFTs of the ΔR_L spectra, and adjacent peak positions. A large side-gate voltage sweep of near 400 mV displays four alternations between $e/2$ and $e/4$ periods: the top trace is the ΔR_L measurement, with vertical line separation there corresponding to $e/2$ and $e/4$ periods as defined by period measurements at filling factors 2, $5/3$, or $7/3$ for each preparation. The middle trace is the FFT amplitude value corresponding to the peak in the FFT spectrum of either $e/2$ (black, labeled $e/2$) or $e/4$ (red, labeled $e/4$) swept over the full side-gate range. The FFT uses a window of roughly 30 mV and progresses at 5 mV steps over the spectrum of the top trace. The FFT values as a function of side-gate voltage show alternation of $e/4$ and $e/2$ periods as the side gate is swept. The bottom trace is the difference in adjacent peak positions for the predominant peaks in each section of either $e/2$ or $e/4$ periods. The aperiodic $e/4$ and $e/2$ alternation can be ascribed to sweeping over a population of localized $e/4$ quasiparticles, alternating an enclosed even-odd number, and expressing the $e/4$ oscillation periods according to the quasiparticle's non-Abelian properties. The figure's schematic depicts this process. $T=25$ mK, current 2 nA, preparation g.

phase with respect to traces A to D. However, in the 175–225 mV sequences six peaks again occur but are out of phase. Note the sections of apparent phase disruption (150–170 mV and 225–245 mV) where assignment of period is not readily possible.

Beyond the properties of the aperiodicity and reproducibility, the general finding²¹ that the $e/2$ oscillations are of smaller amplitude than the $e/4$ is again supported. Another property of the $e/2$ sections apparent in these data is that *within* each section the runs or series of $e/2$ oscillations are

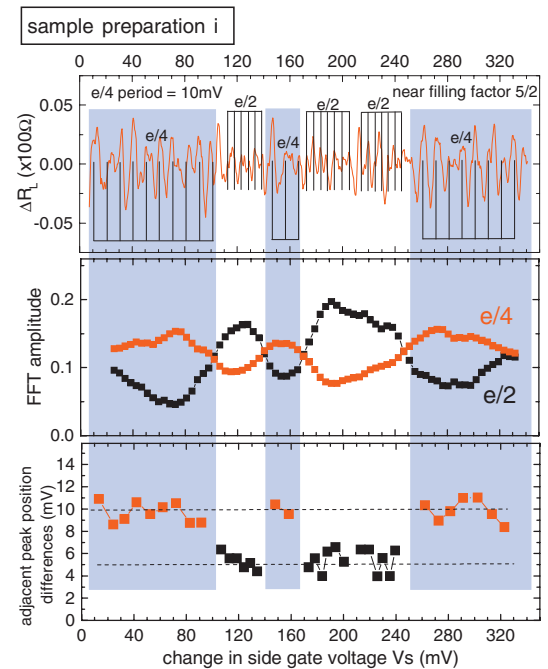
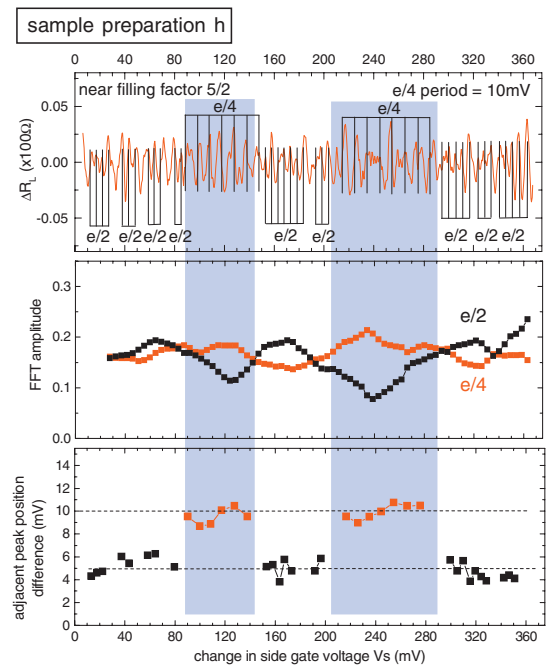


FIG. 6. (Color) Further examples of alternation of $e/4$ and $e/2$ periods over a large side-gate sweep range, demonstrating resolution of $e/4$ and $e/2$ period sections in two sample preparations. For each sample, the ΔR_L measurement is shown in the top trace, scanned FFT over this spectrum is shown in the middle panel, and adjacent peak to peak position differences are shown in the bottom panel for a single sample preparation. As in Fig. 5, the scanned FFT uses a window of approximately 30 mV, with FFT performed at ~ 5 mV increments. The red and black data of the middle panel correspond to FFT amplitude peak values at $e/4$ and $e/2$, respectively, for the window. The normalized $e/4$ and $e/2$ period FFT amplitudes alternate in which is larger over the range of side-gate sweep, corresponding to the $e/4$ and $e/2$ predominance alternation in the data of the bottom and top panels. Measurements taken at temperature=25 mK, 2 nA current; sample preparations h and i.

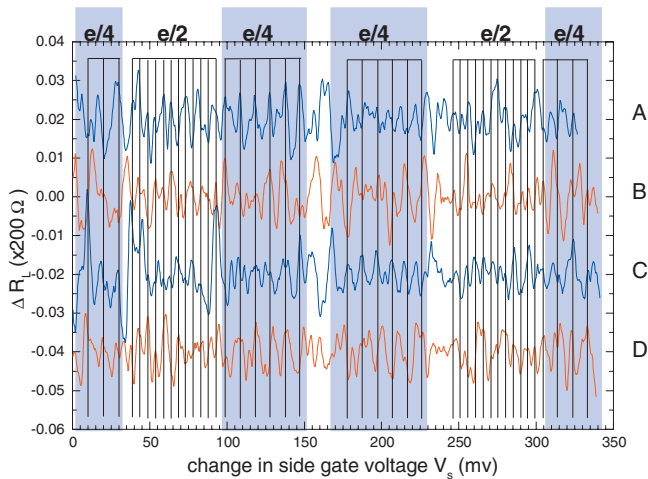


FIG. 7. (Color) Reproducibility of $e/4$ to $e/2$ sequences in longitudinal resistance ΔR_L measurements. Four side-gate voltage sweeps traversing the same total applied side-gate voltage at the same single fixed B field near filling factor $5/2$ are shown in the figure, each from -3.600 to -3.950 V. Each trace A-D corresponds to slow application (~ -15 mV/h) of bias to the channel gate set V_s over the range of the abscissa with similar return rate to the initial bias value. The $e/2$ and $e/4$ periods are marked for comparison between traces, with an error of starting bias of roughly ± 5 mV between traces. Note that the general pattern of the $e/4$ and $e/2$ sequences is reproducible and maintained in some detail between different traces; all four traces show the same oscillation periods of $e/2$ or $e/4$ for a given total side-gate voltage within the error of the applied starting voltage. Some phase disruptions at ~ 160 and ~ 235 mV are present. $T=25$ mK, current 2 nA, sample preparation j.

generally of smaller duration than the $e/4$ runs within a section; the phase disruptions are more prevalent in the $e/2$ sections. These large V_s excursion data demonstrate that alternation of $e/4$ and $e/2$ period oscillations is a dominant feature of the $5/2$ interferometric result, with particular properties exposed that include the aperiodicity and reproducibility of the alternation, and the lower amplitude and smaller oscillation sequences of the $e/2$ versus $e/4$ oscillations.

Again, for a given sample preparation the presence of $e/2$ or $e/4$ oscillation periods is dependent on the value of the voltage applied, V_s : repetition of side-gate scan over the same side-gate voltage values will result in the same alternation pattern with extent of the $e/4$ or $e/2$ sets similar; Fig. 7. This indicates that the presence of $e/4$ or $e/2$ is dependent on the specific area enclosed by the interferometer.

These data of alternating $e/4$ and $e/2$ period oscillations as a function of swept side-gate voltage V_s are consistent with the proposed picture of $5/2$ excitations possessing non-Abelian statistics. In this theory^{16–20} for the excitations of $e/4$ charge traversing an interferometer as used here, a period corresponding to the $e/4$ charge would be expressed for a side-gate voltage sweep where the number of encircled, localized quasiparticles is even and does not change during the sweep. If the encircled number of localized quasiparticles is odd, the $e/4$ oscillations are suppressed due to the non-Abelian nature of the quasiparticles. The data are consistent with this even-odd model. As the side gate is swept over a

large range the number of localized quasiparticles in the enclosed area will change. With this change in number the parity of the enclosed quasiparticle number will necessarily change. The $e/4$ A-B oscillations shown in the data are where an even number of localized quasiparticles is present in the enclosed area. The $e/2$ oscillations experimentally displayed here in alternation with the $e/4$ oscillations represent the encircling of an odd number of quasiparticles within the interferometer area A; the $e/4$ oscillations are suppressed and the smaller amplitude $e/2$ oscillations are now evident. The possible mechanisms for $e/2$ oscillations are described below. More importantly, the alternation presents in the form expected for excursion of the side gate producing alternating even and odd total numbers of enclosed localized quasiparticles. The variation in the range of the gate voltage between switching or alternation back and forth from $e/4$ to $e/2$ is aperiodic or random in side-gate voltage extent, and corresponds to the spatial distribution of localized $e/4$ quasiparticles, which should be random: The pattern of $e/4$ and $e/2$ oscillations provide a “fingerprint” of the quasiparticle localization in the device. It is observed that the patterns of gate sweep extents of $e/4$ and $e/2$ oscillations are reproducible within a sample preparation. This indicates that the localization potential landscape does not change for a given sample preparation, roughly reproducing the sites at which the quasiparticles are localized even as the gate is swept past depletion and repopulation at the localization site.

C. Interchange of $e/4$ and $e/2$ periods with change in magnetic field

We turn now to altering the enclosed quasiparticle number by changing the applied B field. This manipulation of the enclosed localized quasiparticle number between even and odd induces interchange between $e/4$ and $e/2$ A-B oscillation periods.

In these correlated electron systems, changing the applied B field induces a change in the number of quasiparticles in the system, and near a quantum Hall state changes the number of localized quasiparticles. Changing the magnetic field over a sufficiently large range will therefore alter the quasiparticle population within a defined area, altering the parity of the number of quasiparticles between even and odd within that area. As described above, for a particular fixed B -field value, a side-gate sweep shows the aperiodic alternation of $e/4$ and $e/2$ A-B oscillations that reflects the localized quasiparticle population within the area change in the interferometer: the alternation pattern is specific to the particular range of the side-gate sweep. In this purported non-Abelian quasiparticle system, adjusting the applied magnetic field is expected to result in a distinctive change to this alternation pattern:^{16–20} a parity change in the encircled localized quasiparticle number should interchange the $e/4$ and $e/2$ periods. A small B -field adjustment insufficient to add a localized quasiparticle will not change the pattern of aperiodic $e/4$ and $e/2$ observed over the same side-gate sweep. However, a B -field change in sufficient magnitude to produce an odd number change in the localized quasiparticle population of the enclosed area interferometer will have a specific effect;

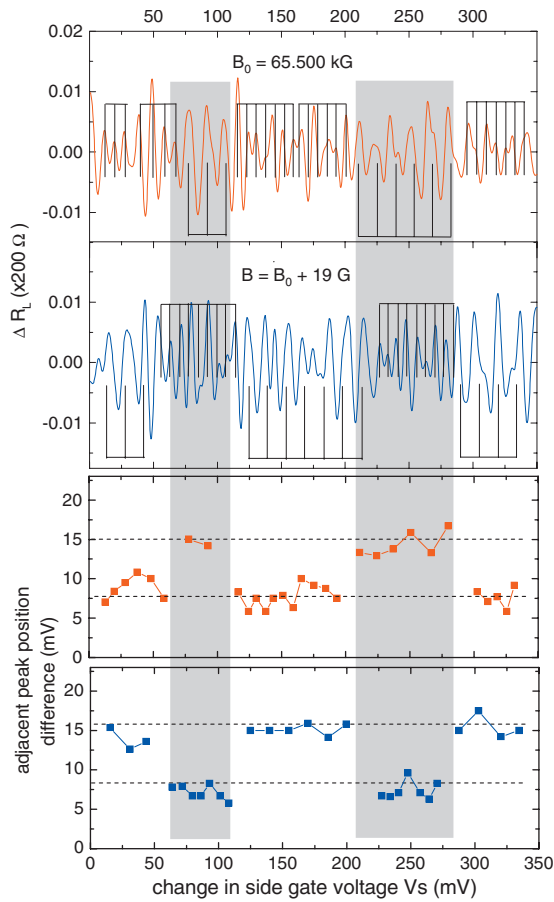


FIG. 8. (Color) B -field-induced interchange of $e/4$ and $e/2$ oscillation sequences near filling factor $5/2$. Top two panels are ΔR_L versus change in side-gate voltage V_s showing A-B oscillations corresponding to charge $e/4$ and $e/2$ periods. The two traces extend over the same side-gate voltage range of -4.00 to -4.35 V but are at different magnetic field values of $B=65.500$ and 65.519 kG. With addition of this small B -field the pattern in the top trace of $e/2$ and $e/4$ periods is replaced with a pattern in which $e/2$ and $e/4$ are interchanged. This interchange of $e/2$ and $e/4$ patterns is further displayed in the bottom two panels where the adjacent peak differences of the top traces are plotted; the interchanges of $e/2$ and $e/4$ occur for all five period sections present in these traces. This change of 19 G can correspond to addition of one or an odd number of quasiparticles to the area of the interferometer, changing the parity of the number of enclosed quasiparticles. For the $e/4$ quasiparticle to be non-Abelian such a change in parity would induce this observed pattern of interchange of the $e/2$ and $e/4$ periods. $T=25$ mK and current= 1 nA, sample preparation k.

the $e/4$ and $e/2$ periods in the alternation patterns should interchange for a side-gate sweep over the same interferometer area.

This interchange of $e/4$ and $e/2$ periods upon changing B field is shown in Fig. 8. The top two panels show standard ΔR_L measurement versus side-gate voltage over the same values of V_s but at two different B -field values, and the bottom two panels are the corresponding adjacent peak position differences. The two B -value data sets show results consistent with the A-B $e/4$ and $e/2$ period alternation demonstrated thus far in this study; four alternations produce patterns of

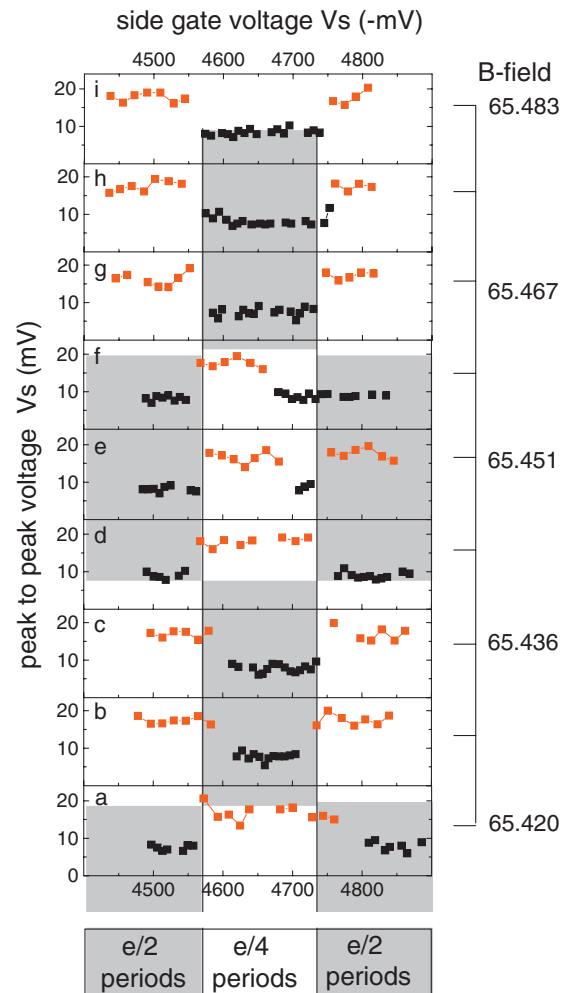


FIG. 9. (Color) Interchange of $e/4$ and $e/2$ period Aharonov-Bohm oscillations near $5/2$ showing the B -field increment that adds one localized $e/4$ quasiparticle to the interferometer. These peak to peak plots are derived from ΔR_L measurements in side-gate sweeps of ~ -4.5 to -4.8 V at nine different B -field values. The B -field values progress in ~ 8 G increments, demonstrating four interchanges of the $e/4$ and $e/2$ periods. The shaded (nonshaded) regions correspond to the presence of predominant $e/2$ ($e/4$) periods. The period of interchange is ~ 20 G, corresponding to the B -field increment necessary to add a single localized $e/4$ quasiparticle to the confinement area, changing the parity of the encircled quasiparticle population. This interchange and the 20 G B -field increment sufficient to induce it are consistent with expected non-Abelian properties of $e/4$ quasiparticles and with the increment calculated using particular parameters of this interferometer at $5/2$; see text. The data are all taken with current= 1 nA and $T=25$ mK, sample preparation l.

five $e/4$ or $e/2$ sections. However, upon the B -field change in 19 G used here interchange of the $e/4$ and $e/2$ periods is induced. Distinct interchange of $e/4$ and $e/2$ periods occurs for all five sections of these A-B oscillations shown in this data with this change in B field. The data support the model that the alternation fingerprint seen with the side-gate sweep can be precisely interchanged in periods by addition of B field.

Further demonstration of period interchange and experimental determination of the B -field change corresponding to addition of a single localized quasiparticle is shown in Fig. 9. Mapped here are ΔR_L vs ΔV_s over the same V_s range for multiple small increments in magnetic field values showing interchange in $e/4$ and $e/2$ at a measurable B -field interval. The value of this interval is checked for agreement with known interferometer parameters at $5/2$ filling, providing a quantitative point of consistency with the model of non-Abelian $e/4$ quasiparticles.

Measurement of the magnetic field change necessary to induce interchange in periods for a specific sample preparation is shown in Fig. 9. This sample preparation is different than that of Fig. 8. In the Fig. 9 data set, a simpler pattern of $e/2$ and $e/4$ alternation [bottom panel a, $e/2$ to $e/4$ to $e/2$] is displayed over the side-gate range of nearly 400 mV. The values of the side-gate excursion are duplicated for the nine B -field values. Here, interchange of the $e/2$ and $e/4$ periods is shown to occur for the first change in B -field value (increase from $B=65.420$). The new $e/2$ and $e/4$ period pattern is maintained upon further increase in B field for the next two values. Reversion to the pattern of the initial B field (panel a) occurs at higher B (above $B=65.436$, panel d). This pattern holds for the next two higher B values, although a small departure from this systematic interchange is noted at B near 65.450 G in the large side-gate voltage range; the source of this anomaly is not presently known. As B field is again increased reversion to the prior pattern is induced (increase above $B=65.459$, panel g). This pattern is sustained for the next several B fields applied. These data show that the $e/2$ and $e/4$ alternation patterns can be interchanged with B -field change; the B -field change necessary to induce the interchange can be extracted from this data. The size of the shaded regions in Fig. 9 roughly delineates similar intervals of $e/4$ or $e/2$ sections, and corresponds to $B \sim 20$ G. This is the interval of B -field change necessary to add a single localized quasiparticle.

This interchange of the alternation patterns induced here by a magnetic field change of $20 \text{ G} = \Delta B$ is quantitatively consistent with that expected for introducing a single localized quasiparticle to this interferometer at filling factor $5/2$: The expected B -field increment necessary to add that quasiparticle to the confinement area A , and so change the parity of the encircled quasiparticle population, is derived as follows. Near filling factor $5/2$ the ratio of electrons to flux quanta is $5/2 = e/\phi_0$, and the expected quasiparticle charge is $e^* = e/4$, or $e = 4e^*$, so that each ϕ_0 corresponds to $10e^* : (1\phi_0)(5e/2\phi_0)(4e^*/e)$ or $0.1\phi_0/e^*$. For the interferometer area $A \sim 0.2 \mu\text{m}^2$ (derived in Ref. 21 and consistent with the gate voltages used here), and magnetic-flux quantum $\phi_0 = 40 \text{ G } \mu\text{m}^2$, the B -field change per quasiparticle is $\Delta\phi_0/e^* = (0.1\phi_0/e^*)(40 \text{ G } \mu\text{m}^2/0.2 \mu\text{m}^2) \sim 20 \text{ G}/e^*$. This number is consistent with the data of Fig. 9 showing multiple $e/4$ and $e/2$ interchanges.

D. Data analysis details

Properties of the data analysis employed in the results section are detailed here. Extraction of oscillatory properties

of R_L data includes fast Fourier transforms of the ΔR_L data and determining adjacent peak position differences, with marking of periods on the ΔR_L data utilizing those methods for extracting periods. The vertical line period markings placed on the ΔR_L data are adjusted in phase to accommodate the series of oscillations present. As noted in previous studies,²¹ oscillation series typically do not present as long continuums of oscillations but instead are usually series of several to many oscillations separated by phase disruptions. The markings placed on the ΔR_L data use the periods derived from the FFTs and from the control measurements at 2 , $5/3$, and $7/3$ but are placed on the data consistent with these phase disruptions. To indicate a continuous series of oscillations, the vertical markings for such a set are linked by a horizontal line and labeled with the appropriate period charge.

FFTs performed on the ΔR_L data are the principal means of extracting the predominant oscillation periods. While used on all filling factor data, for the smaller quasiparticle charge oscillations (larger periods) the minimum range of V_s sweep over which periods could be well determined is limited. It is observed that less than 15 mV V_s range is not viable for extracting oscillation frequencies, and that at 25 mV periods were defined and resolved. This finding sets the limit on swept FFTs (Figs. 5 and 6), and the larger frequency resolution for large V_s extent prompted examining sections of the full V_s scans showing predominant periods on inspection (Fig. 4).

The second analysis method for examining the oscillatory properties in the data uses the differences in adjacent peak positions. Here the peak position in side-gate voltage of a given peak (V_i) is subtracted from the next higher V_s peak position (V_{i+1}), with these values plotted over the full range of the side-gate sweep ($V_{i+1} - V_i$ vs V_i). The predominant peaks within sections ($e/4$ or $e/2$ prevalent periods) of V_s sweep are used, neglecting lower amplitude features. Examples of this are described below.

FFTs are performed on either the full ΔR_L range displayed in each figure or on the range explicitly delineated with each spectrum. The FFT has the advantage that the full spectral weight of $\Delta R_L(V_s)$ is used in each transform. The principal disadvantage to the FFTs is the finite extent of V_s needed to derive a meaningful FFT spectrum so that abrupt changes in oscillatory period are not readily apparent. For assessing prevalent periods the adjacent peak difference method overcomes this limitation in the FFT but does not incorporate the full spectral weight of the data: the peak difference period appears intrinsically noisier than the period definition by FFTs.

Data analysis methods applied to each figure are outlined below. Figure 1: plots of ΔR_L take the measured R_L and subtract the gross background values at that filling factor. FFTs in the insets of (c) and (d) are taken over the entire range of data shown in the respective ΔR_L traces. The FFTs covering the ΔR_L measurement of (e) are taken over the ranges listed on the figure. Figure 4: FFTs in the (ii) panels are extracted from the sections defined in the (i) panels. The adjacent peak positions plot data are derived by subtracting the V_s position of a peak from the V_s position of the next peak at higher V_s . The threshold for defining a peak is larger in the $e/4$ sections than in the $e/2$ sections. An example is

Fig. 4, preparation e, at ~ 85 mV. This peak is not included in the peak differences of panel (iii). For the three data sets of Fig. 4 roughly four such additional features are present within a total of nearly eighty peaks. Figures 5 and 6: the scanned FFT employed here is comprised of FFTs taken of a window roughly 30 mV wide, stepped across the ΔR_L trace at 5 mV increments. The data plotted are the FFT amplitude at the $e/2$ peak frequency position (black, labeled $e/2$) and at the $e/4$ peak frequency position (red, labeled $e/4$) where these positions are determined by the peaks apparent in FFT of the entire ΔR_L spectrum trace. To properly normalize the $e/2$ and $e/4$ amplitudes for the different FFTs, four FFT amplitudes are taken at four different frequencies (mV^{-1}), and their sum is used to normalize the $e/4$ and $e/2$ points. These normalized values are plotted in the (ii) panels after adjacent amplitudes are averaged in each. Figures 7–9: all analysis here is described previously.

IV. DISCUSSION

The finding of alternation of $e/4$ and $e/2$ oscillations as encircled area A is changed and the finding of interchange of $e/4$ and $e/2$ oscillation interference patterns with magnetic field change are as theoretically prescribed for non-Abelian $e/4$ quasiparticles. These interferometric results in tandem are supportive of the conclusion that $e/4$ quasiparticles are non-Abelian.

Before describing a possible full picture of the alternating and interchanging $e/4$ and $e/2$ oscillations, the origin of the $e/2$ oscillations is addressed. The origin of the $e/2$ period is an open issue. Two leading mechanisms for $e/2$ period oscillations are that Abelian $e/2$ charges are present and demonstrate interference or that $e/4$ charge traverses the interferometer twice. Both pictures consider $e/4$ oscillations as A-B oscillations for an even enclosed quasiparticle number, and the $e/2$ oscillations are exposed due to *suppression* of $e/4$ oscillations. Interference by $e/2$ charge quasiparticles may be the preferred model: $e/2$ periods result from the presence of Abelian $e/2$ charge quasiparticles, exposing a fundamental charge in the system.^{26,27} Several recent theoretical studies^{27–30} have discussed the interference processes in these devices and explicitly examined the mechanisms of the $e/2$ oscillations. In the different picture of $e/2$ period due to twice traversal of the area by $e/4$ charge, that quasiparticle must complete two laps around the interferometer, encircling an even quasiparticle number: the total area encircled is doubled, resulting in an $e/2$ period. This mechanism is unlikely given the additional tunneling events at the qpcs which would markedly reduce the $e/2$ oscillation amplitudes.

A probable model for the data is the following. Both non-Abelian $e/4$ charge quasiparticles and Abelian $e/2$ charge quasiparticles are present near $5/2$ filling factor. In the interference measurements a number of $e/4$ quasiparticles are localized within the enclosed area A of the interferometer. This area A changes with side-gate sweep and the number of en-

closed localized quasiparticles changes with sufficiently large side-gate voltage excursion. As the side-gate voltage is swept the $e/4$ period oscillations are expressed when the enclosed localized $e/4$ number is even. When the enclosed number is odd, the $e/4$ period oscillations are suppressed. In either case the non-Abelian $e/4$ charge quasiparticles are encircling the device area A but only express interference for even localized $e/4$ number. The Abelian $e/2$ quasiparticles are likewise encircling the enclosed area A , and can interfere through their two interferometer paths. However, their Abelian statistics dictate that a changing parity of enclosed localized quasiparticles does not change their interference expression: the $e/2$ periods should be present regardless of the number of encircled localized charges. The amplitude of these $e/2$ oscillations is smaller than those of the $e/4$ oscillations when $e/4$ are not suppressed. This amplitude difference means that the $e/4$ periods are dominant when an even number of $e/4$ quasiparticles is enclosed in area A , but when that number is odd, the smaller $e/2$ period oscillations are then observed. This difference in dominance results in an apparent alternation of the $e/4$ and $e/2$ periods. Theoretical modeling of these different amplitude and period oscillations for $e/2$ and $e/4$ results in an alternation pattern consistent with that observed in these experiments.³⁰ This picture is also consistent with the interchange of the $e/4$ and $e/2$ patterns observed with addition of a single localized $e/4$ quasiparticle via change in magnetic field: the B -field change produces a parity switch in the number of localized $e/4$ particles for a given side-gate voltage range, the $e/4$ periods are consequently expressed or suppressed for that range on a background of ever-present small amplitude $e/2$ oscillations.

To conclude, the data presented here show alternating observable $e/4$ and $e/2$ period oscillations that are distinctly consistent with the theory of non-Abelian $e/4$ quasiparticles. The mechanisms of changing area through side-gate voltage or changing B -field produce this alternation and interchange. The alternation reflects the specific even-odd statistical property proposed for non-Abelian $e/4$ quasiparticles. The properties of these oscillations are as expected for the operation of the interferometer where a random spatial distribution of localized quasiparticles is traversed by the side gate. Addition of magnetic flux corresponding to addition of an odd number of localized quasiparticles is consistent with the observed interchange of $e/4$ and $e/2$ period oscillation sequences. The conclusion that $e/4$ quasiparticles are non-Abelian has important ramifications for the utility of this system; $e/4$ excitations are consequently viable candidates for performing topological quantum computation operations.

ACKNOWLEDGMENTS

The authors gratefully acknowledge useful discussions with C. Nayak, B. I. Halperin, A. Stern, D. Natelson, and H. L. Stormer, and also acknowledge technical assistance by M. Peabody.

*Corresponding author; rlw@alcatel-lucent.com

- ¹R. L. Willett, J. P. Eisenstein, H. L. Stormer, D. C. Tsui, A. C. Gossard, and J. H. English, *Phys. Rev. Lett.* **59**, 1776 (1987).
- ²G. Moore and N. Read, *Nucl. Phys. B* **360**, 362 (1991).
- ³F. D. M. Haldane and E. H. Rezayi, *Phys. Rev. Lett.* **60**, 956 (1988).
- ⁴S.-S. Lee, S. Ryu, C. Nayak, and M. P. A. Fisher, *Phys. Rev. Lett.* **99**, 236807 (2007).
- ⁵M. Levin, B. I. Halperin, and B. Rosenow, *Phys. Rev. Lett.* **99**, 236806 (2007).
- ⁶B. Blok and X. G. Wen, *Nucl. Phys. B* **374**, 615 (1992).
- ⁷M. Greiter, X.-G. Wen, and F. Wilczek, *Nucl. Phys. B* **374**, 567 (1992).
- ⁸C. Nayak and F. Wilczek, *Nucl. Phys. B* **479**, 529 (1996).
- ⁹A. Y. Kitaev, *Ann. Phys.* **303**, 2 (2003).
- ¹⁰Daniel Arovas, J. R. Schrieffer, and Frank Wilczek, *Phys. Rev. Lett.* **53**, 722 (1984).
- ¹¹C. de C. Chamon, D. E. Freed, S. A. Kivelson, S. L. Sondhi, and X.-G. Wen, *Phys. Rev. B* **55**, 2331 (1997).
- ¹²S. Kivelson, *Phys. Rev. Lett.* **65**, 3369 (1990).
- ¹³J. K. Jain, S. A. Kivelson, and D. J. Thouless, *Phys. Rev. Lett.* **71**, 3003 (1993).
- ¹⁴F. E. Camino, W. Zhou, and V. J. Goldman, *Phys. Rev. Lett.* **95**, 246802 (2005).
- ¹⁵F. E. Camino, W. Zhou, and V. J. Goldman, *Phys. Rev. Lett.* **98**, 076805 (2007).
- ¹⁶E. Fradkin, C. Nayak, A. Tsvetlik, and F. Wilczek, *Nucl. Phys. B* **516**, 704 (1998).
- ¹⁷A. Stern and B. I. Halperin, *Phys. Rev. Lett.* **96**, 016802 (2006).
- ¹⁸P. Bonderson, A. Kitaev, and K. Shtengel, *Phys. Rev. Lett.* **96**, 016803 (2006).
- ¹⁹S. Das Sarma, M. Freedman, and C. Nayak, *Phys. Rev. Lett.* **94**, 166802 (2005).
- ²⁰W. Bishara and C. Nayak, *Phys. Rev. B* **77**, 165302 (2008).
- ²¹R. L. Willett, L. N. Pfeiffer, and K. W. West, *Proc. Natl. Acad. Sci. U.S.A.* **106**, 8853 (2009).
- ²²M. Dolev, M. Heiblum, V. Umansky, A. Stern, and D. Mahalu, *Nature (London)* **452**, 829 (2008).
- ²³I. Radu, J. B. Miller, C. M. Marcus, M. A. Kastner, L. N. Pfeiffer, and K. W. West, *Science* **320**, 899 (2008).
- ²⁴R. L. Willett, M. J. Manfra, L. N. Pfeiffer, and K. W. West, *Appl. Phys. Lett.* **91**, 052105 (2007).
- ²⁵C. W. J. Beenakker and H. van Houten, *Solid State Physics* (Academic Press, New York, 1991), Vol. 44, p. 1.
- ²⁶Y. Zhang, D. T. McClure, E. M. Levenson-Falk, C. M. Marcus, L. N. Pfeiffer, and K. W. West, *Phys. Rev. B* **79**, 241304(R) (2009).
- ²⁷See X. Wan, Z. Hu, E. Rezayi, and K. Yang, *Phys. Rev. B* **77**, 165316 (2008).
- ²⁸W. Bishara, P. Bonderson, C. Nayak, K. Shtengel, and J. Slingerland, *Phys. Rev. B* **80**, 155303 (2009).
- ²⁹H. Chen, Z. Hu, K. Yang, E. Rezayi, and X. Wan, *Phys. Rev. B* **80**, 235305 (2009).
- ³⁰W. Bishara and C. Nayak, *Phys. Rev. B* **80**, 155304 (2009).